The Astrophysical Journal Supplement Series, 232:12 (8pp), 2017 September https://doi.org/10.3847/1538-4365/aa850a

Non-relativistic Free–Free Emission due to the *n*-distribution of Electrons—Radiative Cooling and Thermally Averaged and Total Gaunt Factors

Miguel A. de Avillez[1,2] and Dieter Breitschwerdt[2]
[1] Department of Mathematics, University of Évora, R. Romão Ramalho 59, 7000 Évora, Portugal; mavillez@galaxy.lca.uevora.pt
[2] Zentrum für Astronomie und Astrophysik, Technische Universität Berlin, Hardenbergstrasse 36, D-10623 Berlin, Germany
Received 2015 August 28; revised 2017 July 4; accepted 2017 July 5; published 2017 September 13

Abstract

Tracking the thermal evolution of plasmas, characterized by an *n*-distribution, using numerical simulations, requires the determination of the emission spectra and of the radiative losses due to free–free emission from the corresponding temperature-averaged and total Gaunt factors. Detailed calculations of the latter are presented and associated with *n*-distributed electrons with the parameter n ranging from 1 (corresponding to the Maxwell–Boltzmann distribution) to 100. The temperature-averaged and total Gaunt factors with decreasing n tend toward those obtained with the Maxwell–Boltzmann distribution. Radiative losses due to free–free emission in a plasma evolving under collisional ionization equilibrium conditions and composed by H, He, C, N, O, Ne, Mg, Si, S, and Fe ions, are presented. These losses decrease with a decrease in the parameter n, reaching a minimum when $n = 1$, and thus converge with the loss of thermal plasma. Tables of the thermal-averaged and total Gaunt factors calculated for *n*-distributions, and a wide range of electron and photon energies, are presented.

Key words: atomic data – atomic processes – ISM: general – plasmas – radio continuum: general – radiation mechanisms: general

Supporting material: tar.gz file

1. Introduction

Non-thermal electron distributions, e.g., κ (Vasyliunas 1968), n (Hares et al. 1979; Seely et al. 1987), depleted high-energy tails (Druyvesteyn 1930; Behringer & Fantz 1994), and hybrid Maxwell–Boltzmann/power-law tails (Berezhko & Ellison 1999; Porquet et al. 2001; Dzifčáková et al. 2011), can occur frequently in the low-density plasma. In principle, this may arise in any place where a high temperature or density gradient exists, or when energy is deposited into the tail of the distribution at a rate that is sufficiently high to overcome the establishment of thermal equilibrium described by the Maxwell–Boltzmann distribution (hereafter MB).

In the astrophysical context, κ- and *n*-distributions have been used to describe the evolution of electrons, e.g., during a solar flare event, and to interpret spectral lines. It is possible that microscopic instabilities like a two-stream or Farley-Buneman instability (Buneman 1963; Farley 1963) can occur under these conditions, which drive the electron distribution strongly into non-equilibrium (Karlický et al. 2012). Events of magnetic reconnection, in which topological field changes force magnetic energy to be released impulsively and dissipated into heat, accompanied by particle acceleration and steep gradients in temperature, should be ubiquitous in the interstellar medium (ISM). However, they can be difficult to observe individually due to the small extension of the regions in which they happen. Hence, observed free–free emission might often contain a contribution from *n*-distribution electrons.

The emission spectra and the radiative losses due to free–free emission by an astrophysical plasma are calculated by means of the temperature-averaged and total free–free Gaunt factor[3] (see discussions in, e.g., Karzas & Latter (1961, hereafter KL1961), Carson (1988), Hummer (1988), Janicki (1990), Sutherland (1998), Nozawa et al. (1998), Itoh et al. (2000), van Hoof et al. (2014), and de Avillez & Breitschwerdt (2015, hereafter AB2015, and references therein).

Here, we continue our previous work (AB2015) by carrying out detailed calculations (and producing look-up tables to be used in any emission software through interpolation) of the non-relativistic temperature-averaged and total free–free Gaunt factors for the interaction of electrons (having an *n*-distribution) with a Coulomb field, which is found, for instance, when electrons interact with ions in an astrophysical plasma.

The structure of this paper is as follows. Section 2 presents the theoretical derivation of the temperature-averaged and total free–free Gaunt factors. Section 3 deals with the methods and results of the present calculations for *n*-distributed electrons. In Section 4 a detailed comparison between our results and those previously published by other authors is made. Section 5 describes the tabulated data, the paper is concluded in Section 6, and final remarks are provided in Section 7.

2. Temperature-averaged and Total Gaunt Factor

The energy emitted per unit time and unit volume by free–free emission from electrons with an energy distribution $f(E)$ is given by (see, e.g., KL1961)

$$\frac{d\Lambda_{\rm ff}}{d\nu} = \frac{8\pi^2}{c^3}\left(\frac{2}{3m_e}\right)^{3/2} e^6 z^2 n_e n_{Z,z} \int_{E_o}^{+\infty} \frac{1}{E^{1/2}} f(E)\, g_{\rm ff} \times \left(\epsilon_i = \frac{E}{z^2 {\rm Ry}},\ \epsilon_f = \frac{E - h\nu}{z^2 {\rm Ry}}\right) dE, \quad (1)$$

where ν is the frequency of the emitted photon, $E_o = h\nu$ is the minimum allowed energy of the electrons in order to emit a photon of frequency ν, m_e is the electron mass, n_e is the electron density, $n_{Z,z}$ is the number density of an ion with

[3] The Gaunt factor is a measure of the quantum mechanical correction to the semiclassical cross section of Kramers (1923).

atomic number Z and ionization stage z, and Ry denotes the Rydberg constant.

The integral on the RHS of (1) is the thermally averaged Gaunt factor, denoted by $\langle g_{\rm ff}(\gamma^2, u)\rangle_{\rm em}$ (with $u = h\nu/k_{\rm B}T$ and $\gamma^2 = z^2{\rm Ry}/k_{\rm B}\ T$), multiplied by a normalization constant $N_{\rm em}$ defined such that $\langle g_{\rm ff}(\gamma^2, u)\rangle_{\rm em} = 1$ when $g_{\rm ff} = 1$. Here, T is the temperature and $k_{\rm B}$ is the Boltzmann constant.

With a suitable change of variables ($x = E/k_{\rm B}T$ and $y = x - u$) the thermally averaged Gaunt factor can be written as

$$\langle g_{\rm ff}(\gamma^2, u)\rangle_{\rm em} = \frac{(k_{\rm B}T)^{1/2}}{N_{\rm em}} \times \int_0^{+\infty} \frac{1}{(y+u)^{1/2}} f[(y+u)k_{\rm B}T] g_{\rm ff} \times \left(\epsilon_i = \frac{y+u}{\gamma^2},\ \epsilon_f = \frac{y}{\gamma^2}\right) dy. \quad (2)$$

2.1. Maxwell–Boltzmann Distribution of Electrons

For the Maxwell–Boltzmann distribution of electrons, (2) becomes

$$\langle g_{\rm ff}(\gamma^2, u)\rangle_{\rm em} = \frac{1}{N_{\rm em}} \frac{2e^{-u}}{\sqrt{\pi}(k_{\rm B}T)^{1/2}} \int_0^{+\infty} e^{-y} g_{\rm ff} \times \left(\epsilon_i = \frac{y+u}{\gamma^2},\ \epsilon_f = \frac{y}{\gamma^2}\right) dy. \quad (3)$$

The boundary condition referred above imposes that $N_{\rm em} = \frac{2e^{-u}}{\sqrt{\pi}(k_{\rm B}T)^{1/2}}$ and therefore

$$\langle g_{\rm ff}(\gamma^2, u)\rangle_{\rm em} = \int_0^{+\infty} e^{-y} g_{\rm ff}\left(\epsilon_i = \frac{y+u}{\gamma^2},\ \epsilon_f = \frac{y}{\gamma^2}\right) dy \quad (4)$$

as defined by, e.g., KL1961. The energy emitted per unit time and unit volume is then given by

$$\frac{d\Lambda_{\rm ff}}{du} = \frac{8\pi^2}{hc^3}\left(\frac{2}{3m_e}\right)^{3/2} e^6 z^2 n_e n_{Z,z}\ k_{\rm B}T \frac{2}{\sqrt{\pi}} \times \frac{e^{-u}}{(k_{\rm B}T)^{1/2}}\ \langle g_{\rm ff}(\gamma^2, u)\rangle_{\rm em}, \quad (5)$$

which can be written as

$$\frac{d\Lambda_{\rm ff}}{du} = C\ z^2 n_e n_{Z,z} T^{1/2} e^{-u}\ \langle g_{\rm ff}(\gamma^2, u)\rangle_{\rm em}, \quad (6)$$

with

$$C = 16\left(\frac{2\pi}{3m_e}\right)^{3/2} \frac{e^6 k_{\rm B}^{1/2}}{hc^3} = 1.4256 \times 10^{-27}\ {\rm erg\ cm^3\ s^{-1}\ K^{-1/2}}.$$

2.2. n-distribution of Electrons

For electrons with an n-distribution (see the Appendix)

$$f(E)dE = \frac{2}{\sqrt{\pi}(k_{\rm B}T)^{3/2}} B_n E^{1/2}\left(\frac{E}{k_{\rm B}T}\right)^{(n-1)/2} e^{-E/k_{\rm B}T} dE, \quad (7)$$

where $B_n = \frac{\sqrt{\pi}}{2\Gamma(n/2+1)}$, the thermally averaged Gaunt factor given by (2), is

$$\langle g_{\rm ff}(\gamma^2, u)\rangle_{\rm em} = \frac{1}{N_{\rm em}} \frac{2e^{-u}}{\sqrt{\pi}(k_{\rm B}T)^{1/2}} B_n \int_0^{+\infty} (y+u)^{(n-1)/2} e^{-y} g_{\rm ff} \times \left(\epsilon_i = \frac{y+u}{\gamma^2},\ \epsilon_f = \frac{y}{\gamma^2}\right) dy. \quad (8)$$

Noting that the incomplete Gamma function (Olver et al. 2010)

$$\Gamma\left(\frac{n+1}{2}, u\right) = e^{-u} \int_0^{+\infty} (y+u)^{(n-1)/2} e^{-y} dy, \quad (9)$$

the boundary condition for the thermally averaged Gaunt factor implies that

$$N_{\rm em} = \frac{2}{\sqrt{\pi}} \frac{B_n}{(k_{\rm B}T)^{1/2}} \Gamma\left(\frac{n+1}{2}, u\right) \quad (10)$$

and

$$\langle g_{\rm ff}(\gamma^2, u)\rangle_{\rm em} = \frac{1}{e^u \Gamma\left(\frac{n+1}{2}, u\right)} \int_0^{+\infty} (y+u)^{(n-1)/2} e^{-y} g_{\rm ff} \times \left(\epsilon_i = \frac{y+u}{\gamma^2},\ \epsilon_f = \frac{y}{\gamma^2}\right) dy. \quad (11)$$

The amount of energy emitted per unit time and unit volume is then given by

$$\frac{d\Lambda_{\rm ff}}{du} = C\ z^2 n_e n_{Z,z} T^{1/2}\ B_n\ \Gamma \times \left(\frac{n+1}{2}, u\right) \langle g_{\rm ff}(\gamma^2, u)\rangle_{\rm em}. \quad (12)$$

2.3. Total Power

Integration of (6) and (12) over the photon frequency spectrum gives the total free–free power associated to an ion (Z, z)

$$\Lambda_{\rm ff}(T) = C\ z^2 n_e n_{Z,z} T^{1/2} \langle g_{\rm ff}(\gamma^2)\rangle\ {\rm erg\ cm^{-3}\ s^{-1}}, \quad (13)$$

where $\langle g_{\rm ff}(\gamma^2)\rangle$ is the total free–free Gaunt factor given by

$$\langle g_{\rm ff}(\gamma^2)\rangle = \int_0^{+\infty} e^{-u}\ \langle g_{\rm ff}(\gamma^2, u)\rangle_{\rm em}\ du \quad (14)$$

for the Maxwell–Boltzmann distribution and

$$\langle g_{\rm ff}(\gamma^2)\rangle = B_n \int_0^{+\infty} \langle g_{\rm ff}(\gamma^2, u)\rangle_{\rm em}\ \Gamma\left(\frac{n+1}{2}, u\right) du \quad (15)$$

for the n-distribution of electrons.

From (11) and (15) with $n = 1$ and noting that $\Gamma(1, u) = e^{-u}$ and $B_1 = 1$, both the thermally averaged and the total free–free Gaunt factors for a Maxwellian distribution of electrons are recovered.

2.4. Photoemission versus Photoabsorption

Similar to the definition for the thermally averaged Gaunt factors for photoemission, we can define the thermally

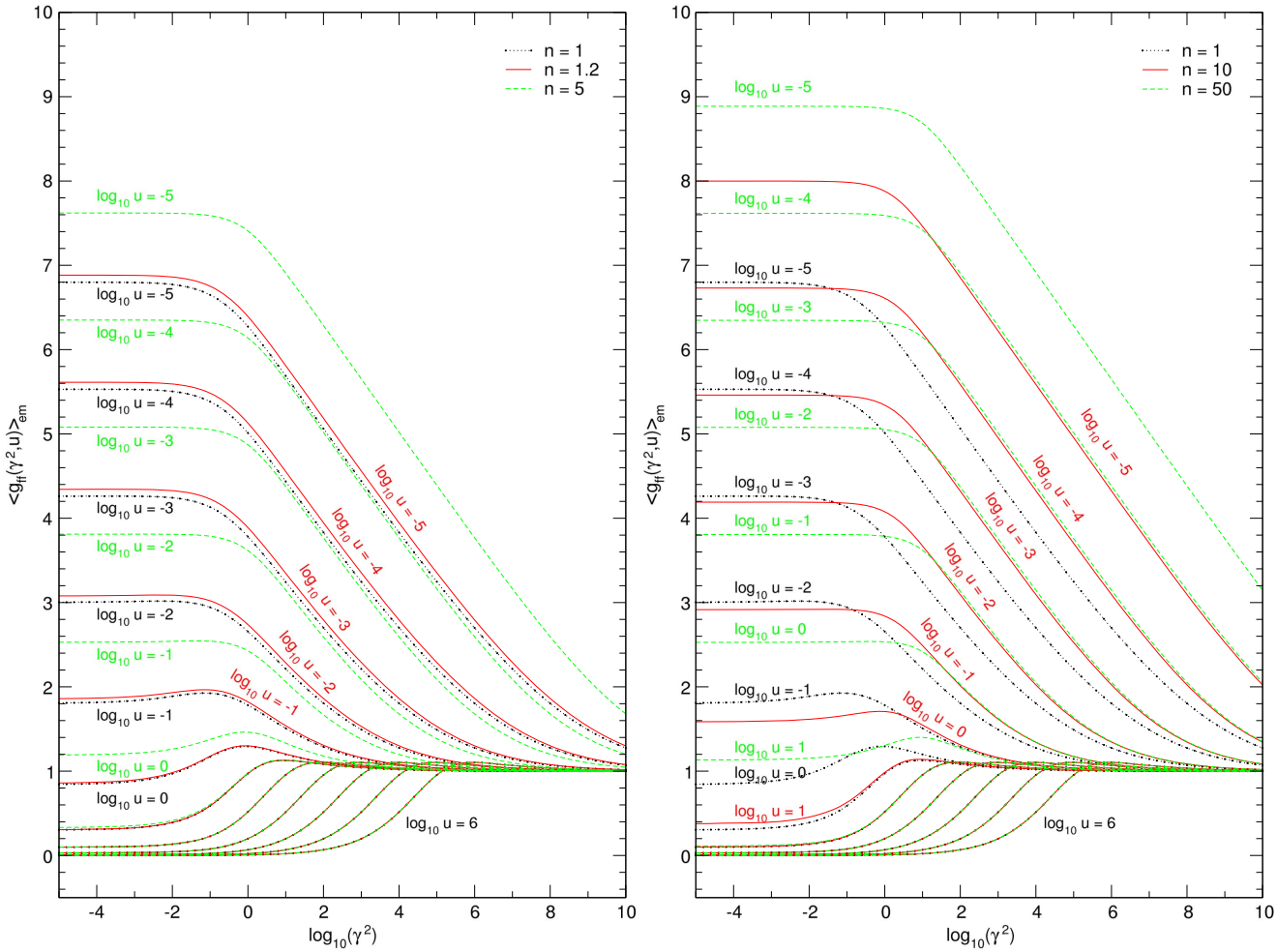

Figure 1. Thermally averaged Gaunt factors for electrons with an n-distribution with $n = 1$, 1.2, and 5 (left panel), and $n = 1$, 10, and 50 (right panel). The curves are displayed for $\log_{10}(u)$, varying from -5 to 6 from top to bottom in each panel.

averaged Gaunt factor for photoabsorption as

$$\langle g_{\rm ff}(\gamma^2, u)\rangle_a = \frac{1}{N_a}\int_0^{+\infty} \frac{1}{E^{1/2}} f(E)\, g_{\rm ff} \times \left(\epsilon_i = \frac{E}{z^2 {\rm Ry}},\, \epsilon_f = \frac{E + h\nu}{z^2 {\rm Ry}}\right) dE, \quad (16)$$

with N_a being the normalization coefficient determined by the boundary condition $\langle g_{\rm ff}(\gamma^2, u)\rangle_a = 1$ when $g_{\rm ff} = 1$. Using the change of variables $x = E/k_{\rm B}T$ and after determining the normalization coefficient, the thermally averaged Gaunt factor for photoabsorption is given by

$$\langle g_{\rm ff}(\gamma^2, u)\rangle_a = \int_0^{+\infty} e^{-x} g_{\rm ff}\left(\epsilon_i = \frac{x}{\gamma^2},\, \epsilon_f = \frac{x + u}{\gamma^2}\right) dx \quad (17)$$

for the Maxwell–Boltzmann distribution and

$$\langle g_{\rm ff}(\gamma^2, u)\rangle_a = \frac{1}{\Gamma\left(\frac{n+1}{2}\right)}\int_0^{+\infty} x^{(n-1)/2} e^{-x} g_{\rm ff} \times \left(\epsilon_i = \frac{x}{\gamma^2},\, \epsilon_f = \frac{x + u}{\gamma^2}\right) dx \quad (18)$$

for the n-distribution. The Maxwellian temperature-averaged Gaunt factors for photoemission and photoabsorption, Equations (4) and (17), yield the same result. This is a consequence of the principle of detailed balance that is required for thermodynamic equilibrium to be reached (see, e.g., Armstrong 1971), a condition that is not verified for the n-distribution with $n > 1$. Thus, Equations (11) and (18) have different results.

3. Calculations and Results

We calculated numerically the temperature-averaged, $\langle g_{\rm ff}(\gamma^2, u)\rangle_{\rm em}$, and total, $\langle g_{\rm ff}(\gamma^2)\rangle$, free–free Gaunt factors for an n-distribution of electrons (n ranging from 1 (Maxwell–Boltzmann distribution) to 100) for $\gamma^2 \in [10^{-5}, 10^{10}]$ and $u \in [10^{-12}, 10^{11}]$ using the Gaunt factors associated with free–free absorption by an electron in the presence of a Coulomb field of an ion. For completeness, the range in γ^2 is limited to 10^{-5}, corresponding to an upper temperature of $T_e/Z^2 = 1.578 \times 10^{10}$ K, although at this temperature relativistic effects are seen and electron–electron bremsstrahlung dominates (see, e.g., Itoh et al. 1985).

The calculations proceeded as follows. First, the free–free Gaunt factors for the absorption of photons of frequency $h\nu$ by

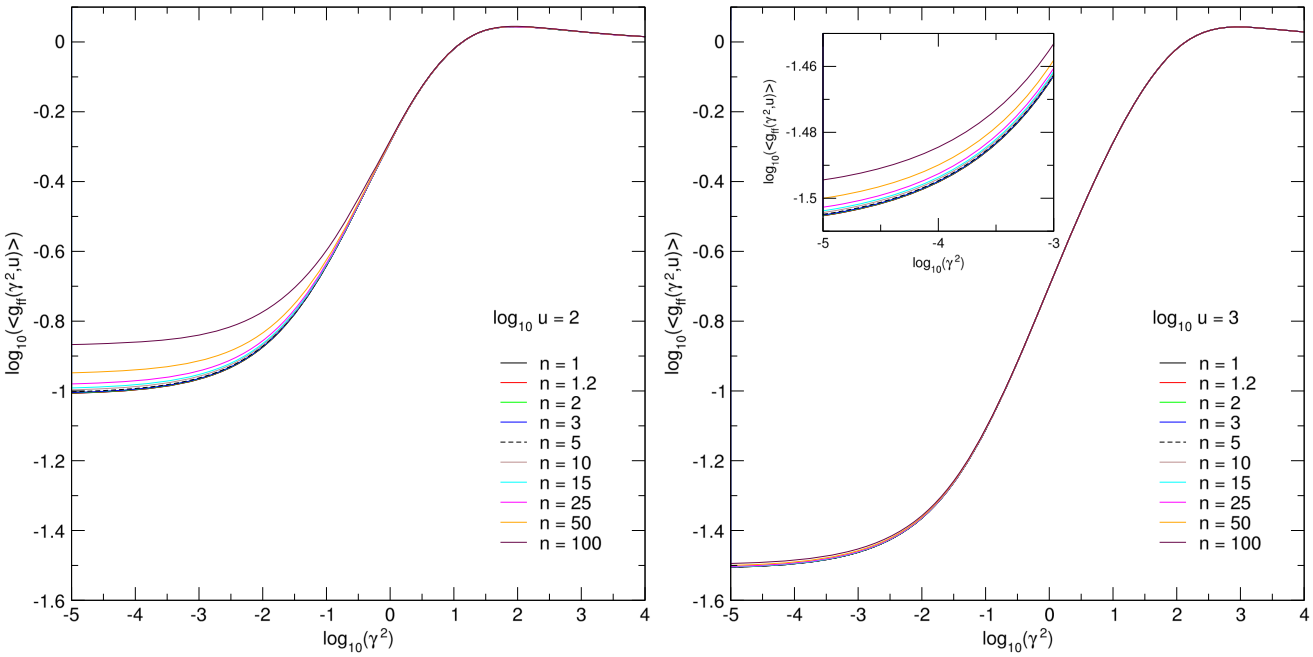

Figure 2. Details of the thermally averaged Gaunt factors (in logarithmic scale) for electrons with an n-distribution (n varying from 1 to 100) as a function of γ^2 for $\log_{10} u = 2$ and 3. Although it appears from the previous figure that $\langle g_{\rm ff}(\gamma^2, u)\rangle_{\rm em}$ overlaps for $\log_{10} u > 1$, there are still small differences at $\log_{10} u = 3$ for $\gamma^2 < 0$ (inset plot in the right panel).

electrons with a range of possible initial energies E_i were explicitly calculated (see AB2015), followed by the determination of the temperature-averaged and total Gaunt factors (Equations (4) and (6), respectively). The Gaunt factor calculation involved double- and quadruple precisions (see the discussion in AB2015), while the numerical integrations were performed with a precision of 10^{-15} using the double-exponential over the semi-finite interval method of Takahasi & Mori (1974) and Mori & Sugihara (2001). We use a modified version (parallelized version) of the Numerical Automatic Integrator for Improper Integral package developed by T. Ooura.[4]

Figure 1 displays the temperature-averaged Gaunt factors calculated for electrons with an n-distribution with $n = 1$ (displayed in the two panels by black dotted lines), 1.2, 5, 10, and 50. The curves are displayed for $\log_{10}(u)$, varying from -5 to 6 from top to bottom in each panel, although our calculations consider a wider range in n, γ^2, and u (see Section 5). Figure 2 details $\langle g_{\rm ff}(\gamma^2, u)\rangle_{\rm em}$ as a function of γ^2 for $\log_{10} u = 2$ (left panel) and 3 (right panel) in a logarithmic scale to show the deviations of $\langle g_{\rm ff}(\gamma^2, u)\rangle_{\rm em}$ for different n at these frequencies.

The temperature-averaged Gaunt factors for $n > 1$ deviate from those calculated for the Maxwell–Boltzmann distribution ($n = 1$). As n increases, the deviations increase with the decrease of $\log_{10} u$ (Figure 1). For $\log_{10} u > 1$ $\langle g_{\rm ff}(\gamma^2, u)\rangle_{\rm em}$ converges to the Maxwell–Boltzmann value (Figure 1), overlapping it when $\log_{10} u > 3$. There are still small differences at $\log_{10} u = 3$ for $\gamma^2 < 0$ (Figure 2).

Figure 3 displays the total Gaunt factor, $\langle g_{\rm ff}(\gamma^2)\rangle$, variation with γ^2 calculated for $n = 1$, 1.2, 2, 3, 5, and 10 (bottom panel) and 15, 25, 50, and 100 (top panel). For each n the total Gaunt factor has a similar profile as $n = 1$ but with the peak shifted to the right. In addition, and as expected from the thermally averaged Gaunt factors' evolutions with γ^2, $\langle g_{\rm ff}(\gamma^2)\rangle$ increases with increasing n.

[4] http://www.kurims.kyoto-u.ac.jp/~ooura/intde.html

4. Validation of the Maxwellian Thermally Averaged and Total Gaunt Factors

In order to validate our results, we carried out a detailed comparison of the temperature-averaged and total free–free Gaunt factors, calculated for electrons with a Maxwellian temperature, with those published by van Hoof et al. (2014). The top panels ofFigures 4 and 5 compare the temperature-averaged and total free–free Gaunt factors determined for the Maxwell–Boltzmann distribution in the present work (red dots) and those calculated by van Hoof et al. (2014, solid lines).

The bottom panel of Figure 4 displays the relative difference between the two calculations of the temperature-averaged Gaunt factor in the ranges $-5 \leqslant \log(\gamma^2) \leqslant 6$ and $-5 \leqslant \log(u) \leqslant 4$. At first sight there seems to be no variation between the solid lines and the dots overlaying them. In fact, the two calculations have relative differences (in percentage) smaller than 0.12% for $\log(u) = -5$ and -4 and smaller than 0.04% for $\log(u) \geqslant -1$. The relative difference between the total Gaunt factors obtained in the two calculations is smaller than 0.233% (bottom panel of Figure 5).

These relative differences result from the different numerical techniques for calculating the hypergeometric functions and machine precision adopted for the calculations of the Gaunt factors (see the discussions in the abovementioned papers and in AB2015), as well as the adopted integrating method used in the calculations of the thermally averaged and total Gaunt factors. While in the present work the double-exponential quadrature method extended to any real function (Mori & Sugihara 2001) was used to calculate the different integrals, van Hoof et al. used an adaptive step-size algorithm for the

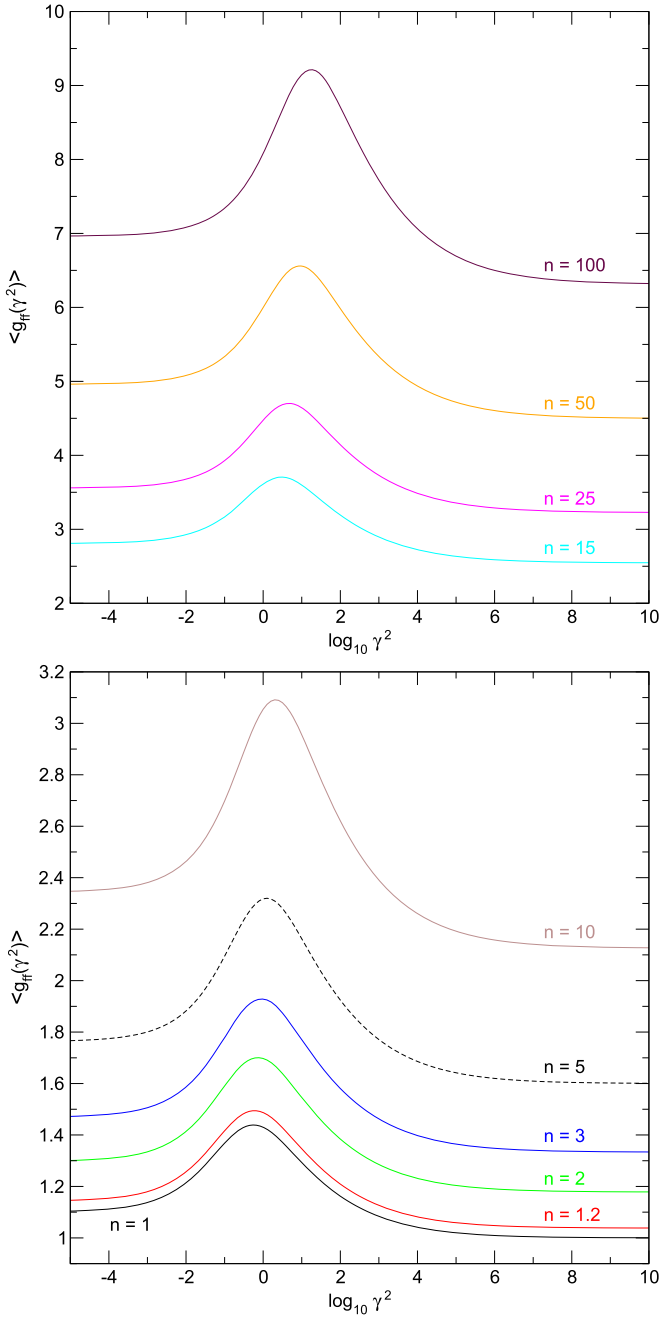

Figure 3. Total free–free Gaunt factor calculated for the n-distributed electrons with $n = 1$, 1.2, 2, 3, 5, and 10 (bottom panel) and $n = 15$, 25, 50, and 100 (top panel). With increasing n, the total Gaunt increases and its peak maximum moves to the right.

integrations, with an estimate of the remainder of the integral to infinity being smaller than 10^{-7} times the total integral up to that point. The relative differences shown above are indicative of the adequacy of our results.

5. Tables

In the supplementary material tar.gz archive, a set of 11 tables referring to the temperature-averaged ($\langle g_{\rm ff}(\gamma^2, u)\rangle_{\rm em}$ versus γ^2 for different u) and the total ($g_{\rm ff}(\gamma^2)$ versus γ^2) free–free Gaunt factor is provided. The parameter space comprises $1 \leqslant n \leqslant 100$, $\gamma^2 \in [10^{-5}, 10^{10}]$, and $u \in [10^{-12}, 10^{11}]$.

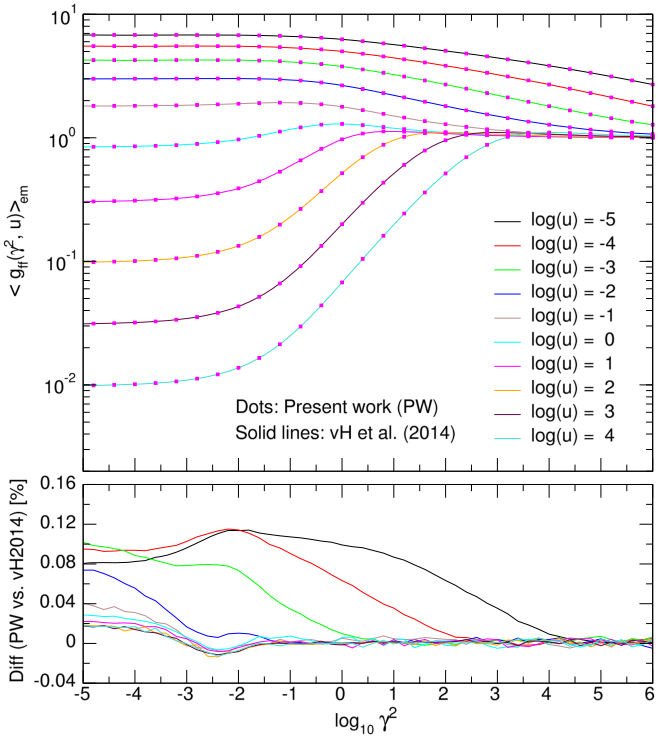

Figure 4. Top panel: comparison between the temperature-averaged free–free Gaunt factors for a thermal distribution of electrons published by van Hoof et al. (2014, solid lines) and those calculated in the present work (magenta dots). Bottom panel: relative differences between the temperature-averaged Gaunt factors obtained in the present work and those of van Hoof et al. (2014).

6. Application to an Optically thin Plasma

We calculated the electron–ion[5] free–free contribution to the radiative losses of a plasma composed of H, He, C, N, O, Ne, Mg, Si, S, and Fe and having solar abundances (Asplund et al. 2009) by considering the evolution of a gas parcel freely cooling from 10^9 K and evolving under collisional ionization equilibrium (CIE). In addition to the free–free emission, the other physical processes included in this calculation comprise electron impact ionization, inner-shell excitation, auto-ionization, radiative, and dielectronic recombination. The internal energy of the gas parcel includes the contributions due to the thermal translational energy plus the energy stored in ionization.

The atomic data used in the present calculations include the electron impact ionization cross sections discussed in Dere (2007) and those available in the Chianti database (see, e.g., Dere et al. 2009). From these cross sections we calculate the ionization rates associated with an ion of atomic number Z and ionic charge z by averaging the product $\sigma(E)v$ over the impacting particle kinetic energy distribution $f(E)$

$$\langle \sigma v \rangle = \int_{I_{Z,z}}^{+\infty} \sigma(E)(2E/m_e)^{1/2} f(E) dE \ \ {\rm cm^3\ s^{-1}}, \qquad (19)$$

where m_e is the electron mass, and $I_{Z,z}$ is the threshold energy in eV.

The radiative and dielectronic recombination rates for the n-distribution are calculated from the fit coefficients to the

[5] Note that electron–electron bremsstrahlung, although important at 10^9 K, is not included in the present calculation.

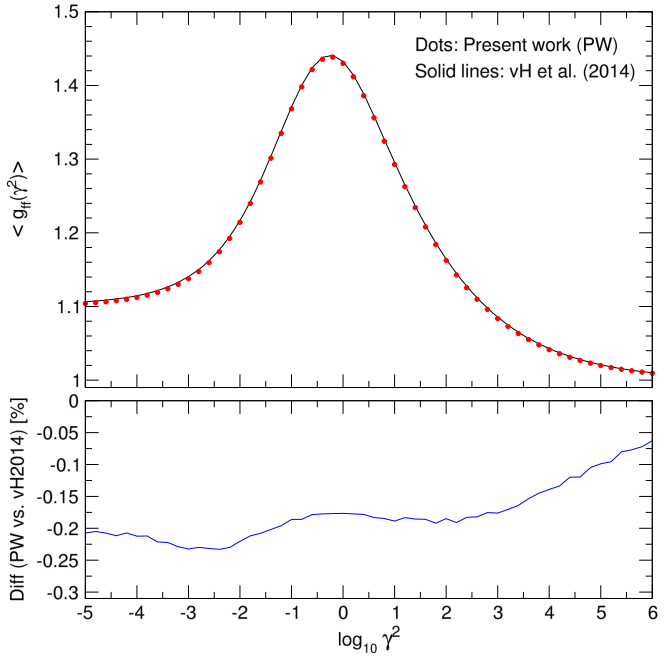

Figure 5. Top panel: comparison of the total free–free Gaunt factors for a thermal distribution of electrons calculated in the present work (red dots) with those pf van Hoof et al. (2014; black line). Bottom panel: relative difference between the total Gaunt factor obtained in the present work and those of van Hoof et al. (2014).

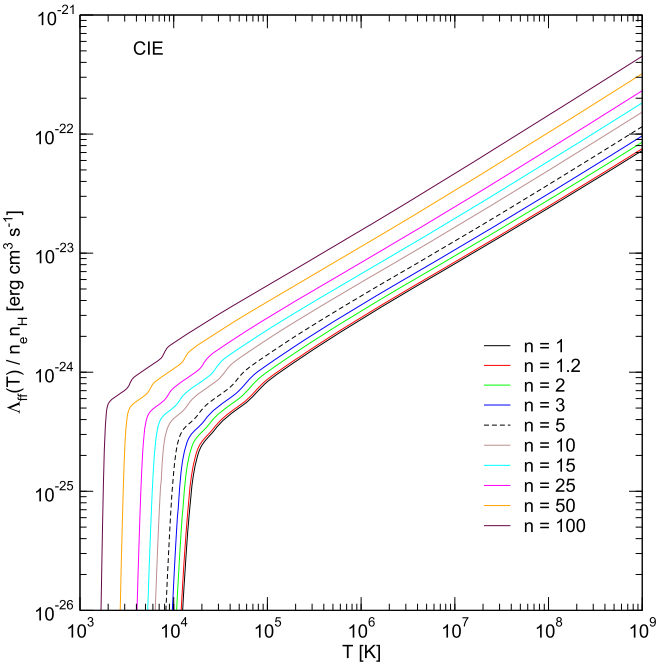

Figure 6. Normalized (to $n_e n_H$) radiative losses due to free–free emission by an optically thin plasma evolving under collisional ionization equilibrium and for electrons having n-distributions ($n = 1$, 1.2, 2, 3, 5, 10, 15, 25, 50, and 100).

Maxwellian rates (Dzifčáková 1998), that is, the radiative recombination rates for the n-distribution are determined from

$$\alpha_{\rm RR}^{n} = \alpha_{Z,z}^{\rm MB} B_n \frac{\Gamma(n/2 - \eta + 1)}{\Gamma(3/2 - \eta)}, \quad (20)$$

where $\alpha_{\rm RR}^{\rm MB}$ is the Maxwellian radiative recombination rate, and η is a parameter of the power-law fit of the Maxwellian rate (see, e.g., Woods et al. 1981)

$$\alpha_{\rm RR}^{\rm MB} = A_{\rm rad}\left(\frac{T}{10^4{\rm K}}\right)^{-\eta} \ {\rm cm^3\ s^{-1}}. \quad (21)$$

The dielectronic recombination rates for the n-distribution of electrons are determined from coefficients of the Maxwellian rates given by the Burgess (1965) general formula,

$$\alpha_{\rm DR}^{\rm MB} = \frac{1}{(k_{\rm B}T)^{3/2}} \sum_j c_j e^{-E_j/(k_{\rm B}T)} \ {\rm cm^3\ s^{-1}}, \quad (22)$$

through (Dzifčáková 1998)

$$\alpha_{\rm DR}^{n} = \frac{B_n}{(k_{\rm B}T)^{3/2}} \sum_j c_j \left(\frac{E_j}{k_{\rm B}T}\right)^{(n-1)/2} e^{-E_j/(k_{\rm B}T)} \ {\rm cm^3\ s^{-1}}. \quad (23)$$

The Maxwellian radiative recombination rate coefficients are taken from Badnell (2006a) [6] for all bare nuclei through Na-like ions recombining to H through Mg-like ions, Altun et al. (2007) for Mg-like ions, Abdel-Naby et al. (2012) for Al-like ions, Nikolić et al. (2010) for Ar-like ions, and Badnell (2006b) for Fe XIII-Fe X ions. The Maxwellian dielectronic recombination rates are taken from Badnell (2006c) for H-like ions, Bautista & Badnell (2007) for He-like ions, Colgan et al. (2004, 2003) for Li and Be-like ions, Altun et al. (2004, 2006, 2007) for B,[7] Na, and Mg-like ions, Zatsarinny et al. (2003, 2004a, 2004b, 2006) for C,[8] O,[9] F, and Ne-like ions, Mitnik & Badnell (2004) for N-like ions, Abdel-Naby et al. (2012) for Al-like ions, and Nikolić et al. (2010) for Ar-like ions. Radiative and dielectronic recombination rates for S II, S III, and Fe VII are adopted from Mazzotta et al. (1998), while for the remaining ions we adopt the radiative and dielectronic recombination rates derived with the unified electron–ion recombination method (Nahar & Pradhan 1994) and those available at NORAD-Atomic-Data.[10]

The calculation was carried out with the Collisional + Photo Ionization Plasma Emission Software (CPIPES; M. A. de Avillez 2017, in preparation), which is a complete rewrite of the E+AMPEC code (de Avillez et al. 2012). The ionization structures due to the 102 ions and 10 atoms (for a total of 112 linear equations) of the gas parcel evolving under CIE conditions were calculated at each temperature using a Gauss elimination method with scaled partial pivoting (Cheney & Kincaid 2008) and a tolerance of 10^{-15}. Having calculated the ionization structure of the gas parcel at each temperature, the losses of energy due to free–free emission were calculated using Equation (7) and assuming the hydrogenic approximation.

Figure 6 displays the free–free emission resulting from the CIE calculation for electrons described by the n-distribution with n ranging from 1 (Maxwell–Boltzmann distribution) through 100. The free–free emission increases with n as expected from the variation of the total Gaunt factor with n as shown in

[6] amdpp.phys.strath.ac.uk/tamoc/DATA/

[7] For Ne VI and Mg VII we use the erratum; Altun et al. (2005).

[8] For N II we follow the erratum Zatsarinny et al. (2005a).

[9] For Ne III, Mg V, and Fe XIX we use the erratum Zatsarinny et al. (2005b).

[10] http://www.astronomy.ohio-state.edu/~nahar

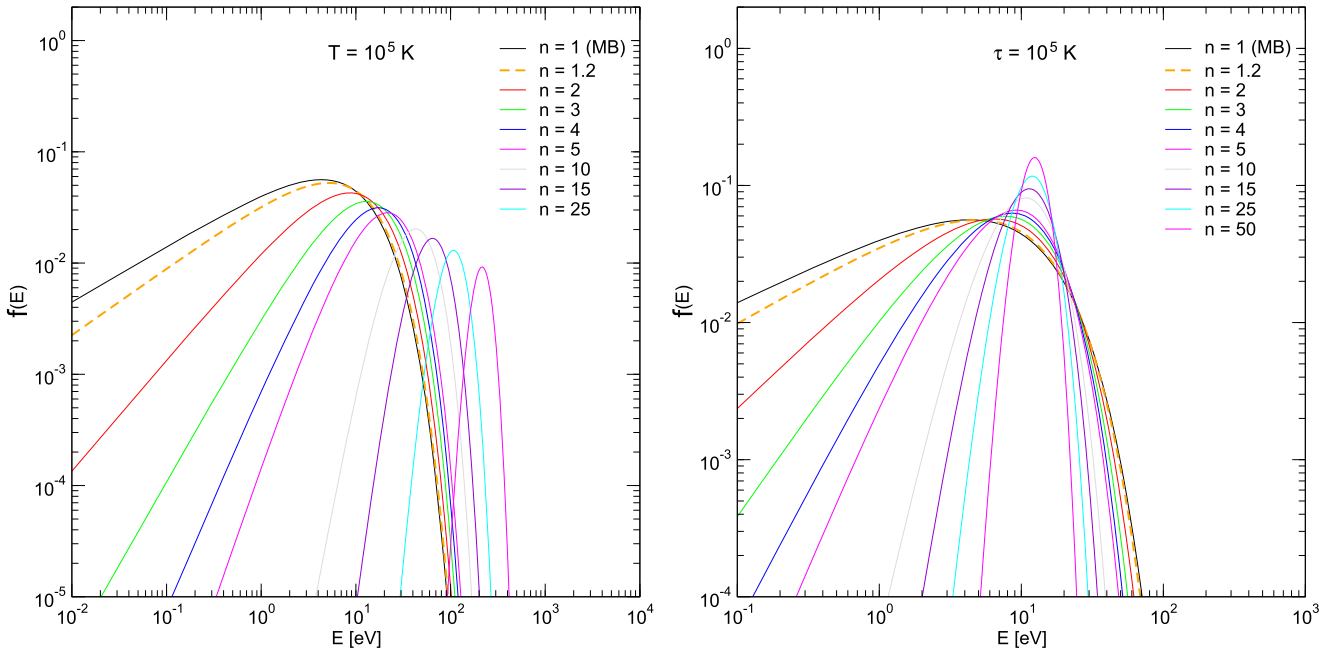

Figure 7. Maxwell–Boltzmann ($n = 1$) and n-distributions (with $n = 1.2$ through 50) at the same temperature ($T = 10^5$ K; left panel) and same pseudo-temperature ($\tau = 10^5$ K; right panel). The $n > 1$ distributions have a steeper high-energy tail than the MB distribution.

Figure 3. This loss of radiation has its minimum when electrons relax to thermal equilibrium, that is, when n becomes 1.

7. Final Remarks

We carried out a detailed calculation of the temperature-averaged and total free–free Gaunt factors that are useful for the determination of the free–free emission power spectrum and losses of radiation in astrophysical plasmas. Bremsstrahlung is in many situations the most important electromagnetic information we can obtain, e.g., in clusters of galaxies with plasma temperatures in the keV range. It is well-known that galaxy cluster or group mergers can generate large-scale shock waves (see, e.g., Russell et al. 2014) and/or high temperature gradients at the interface of different intracluster gases, both of which could drive the electron population, responsible for the emission, out of equilibrium. It is therefore desirable to provide tables of free–free Gaunt factors over a wide range in temperatures for a variety of n-distributions.

We acknowledge the useful comments by the anonymous referee. This research was supported by the project "Hybrid computing using accelerators and coprocessors-modeling nature with a novel approach" (PI: M.A.) funded by the InAlentejo program, CCDRA, Portugal. Partial support for M.A. and D.B. was provided by the *DeutscheForschungsgemeinschaft*, DFG project ISM-SPP 1573. The computations were carried out with the ISM/SKA Xeon Phi supercomputer of the Computational Astrophysics Group, University of Évora.

Appendix
The n-distribution

The n-distribution has a steeper decrease at the high-energy tail than the Maxwell–Boltzmann (MB) distribution, which in turn is an n-distribution with $n = 1$. In energy space, the distribution has the analytical form

$$f_n(E)dE = \frac{2}{\sqrt{\pi}(k_{\rm B}T)^{3/2}} B_n E^{1/2}\left(\frac{E}{k_{\rm B}T}\right)^{(n-1)/2} e^{-E/k_{\rm B}T}dE, \tag{24}$$

where $B_n = \frac{\sqrt{\pi}}{2\Gamma(n/2+1)}$, E is the electron energy, $k_{\rm B}$ is the Boltzmann constant, Γ is the Gamma function, and $n \in [1, +\infty]$ and T are the parameters of the distribution. When $n = 1$ the MB distribution is recovered. The mean energy of the distribution is given by

$$\langle E\rangle = \frac{3}{2}k_{\rm B}\tau, \tag{25}$$

where $\tau = \frac{n+2}{3}T$ is the pseudo-temperature, meaning that it is the temperature of the MB distribution with the same mean energy as the mean energy of the n-distribution; thus, τ has the same physical meaning as T in the MB distribution. Figure 7 compares the n-distribution for different n values with the MB for the same parameter T (top panel) and τ (bottom panel).

The n-distributions with the same τ have higher and narrower peaks than the MB distributions, that is, they have less electrons with both high and low energies, but have an increased number of electrons with intermediate energies.

References

Abdel-Naby, S. A., Nikolić, D., Gorczyca, T. W., Korista, K. T., & Badnell, N. R. 2012, A&A, 537, A40
Altun, Z., Yumak, A., Badnell, N. R., Colgan, J., & Pindzola, M. S. 2004, A&A, 420, 775
Altun, Z., Yumak, A., Badnell, N. R., Colgan, J., & Pindzola, M. S. 2005, A&A, 433, 395
Altun, Z., Yumak, A., Badnell, N. R., Loch, S. D., & Pindzola, M. S. 2006, A&A, 447, 1165
Altun, Z., Yumak, A., Yavuz, I., et al. 2007, A&A, 474, 1051
Armstrong, B. H. 1971, JQSRT, 11, 1731
Asplund, M., Grevesse, N., Sauval, A. J., & Scott, P. 2009, ARA&A, 47, 481

Badnell, N. R. 2006a, ApJS, 167, 334
Badnell, N. R. 2006b, ApJL, 651, L73
Badnell, N. R. 2006c, A&A, 447, 389
Bautista, M. A., & Badnell, N. R. 2007, A&A, 466, 755
Behringer, K., & Fantz, U. 1994, JPhD, 27, 2128
Berezhko, E. G., & Ellison, D. C. 1999, ApJ, 526, 385
Buneman, O. 1963, PhRvL, 10, 285
Burgess, A. 1965, ApJ, 141, 1588
Carson, T. R. 1988, A&A, 189, 319
Cheney, W., & Kincaid, D. 2008, Numerical Mathematics and Computing (6th ed.; Belmont, CA: Thomson Brooks/Cole)
Colgan, J., Pindzola, M. S., & Badnell, N. R. 2004, A&A, 417, 1183
Colgan, J., Pindzola, M. S., Whiteford, A. D., & Badnell, N. R. 2003, A&A, 412, 597
de Avillez, M. A., & Breitschwerdt, D. 2015, A&A, 580, A124
de Avillez, M. A., Spitoni, E., & Breitschwerdt, D. 2012, in ASP Conf. Ser. 453, Advances in Computational Astrophysics: Methods, Tools, and Outcome, ed. R. Capuzzo-Dolcetta, M. Limongi, & A. Tornambè (San Francisco, CA: ASP), 341
Dere, K. P. 2007, A&A, 466, 771
Dere, K. P., Landi, E., Young, P. R., et al. 2009, A&A, 498, 915
Druyvesteyn, M. J. 1930, ZPhy, 64, 781
Dzifčáková, E. 1998, SoPh, 178, 317
Dzifčáková, E., Homola, M., & Dudík, J. 2011, A&A, 531, A111
Farley, D. T. 1963, PhRvL, 10, 279
Hares, J. D., Kilkenny, J. D., Key, M. H., & Lunney, J. G. 1979, PhRvL, 42, 1216
Hummer, D. G. 1988, ApJ, 327, 477
Itoh, N., Nakagawa, M., & Kohyama, Y. 1985, ApJ, 294, 17
Itoh, N., Sakamoto, T., Kusano, S., Nozawa, S., & Kohyama, Y. 2000, ApJS, 128, 125
Janicki, C. 1990, CoPhC, 60, 281
Karlický, M., Dzifčáková, E., & Dudík, J. 2012, A&A, 537, A36
Karzas, W. J., & Latter, R. 1961, ApJS, 6, 167
Kramers, H. A. 1923, PMag, 46, 836
Mazzotta, P., Mazzitelli, G., Colafrancesco, S., & Vittorio, N. 1998, A&AS, 133, 403
Mitnik, D. M., & Badnell, N. R. 2004, A&A, 425, 1153
Mori, M., & Sugihara, M. 2001, JCoAM, 127, 287
Nahar, S. N., & Pradhan, A. K. 1994, PhRvA, 49, 1816
Nikolić, D., Gorczyca, T. W., Korista, K. T., & Badnell, N. R. 2010, A&A, 516, A97
Nozawa, S., Itoh, N., & Kohyama, Y. 1998, ApJ, 507, 530
Olver, F. W. J., Lozier, D. W., Boisvert, R. F., & Clark, C. W. 2010, NIST Handbook of Mathematical Functions (Cambridge: Cambridge Univ. Press)
Porquet, D., Arnaud, M., & Decourchelle, A. 2001, A&A, 373, 1110
Russell, H. R., Fabian, A. C., McNamara, B. R., et al. 2014, MNRAS, 444, 629
Seely, J. F., Feldman, U., & Doschek, G. A. 1987, ApJ, 319, 541
Sutherland, R. S. 1998, MNRAS, 300, 321
Takahasi, H., & Mori, M. 1974, Pub. Res. Inst. Math. Sci., 9, 721
van Hoof, P. A. M., Williams, R. J. R., Volk, K., et al. 2014, MNRAS, 444, 420
Vasyliunas, V. M. 1968, in Physics of the Magnetosphere, ed. R. D. L. Carovillano & J. F. McClay, 622
Woods, D. T., Shull, J. M., & Sarazin, C. L. 1981, ApJ, 249, 399
Zatsarinny, O., Gorczyca, T. W., Fu, J., et al. 2006, A&A, 447, 379
Zatsarinny, O., Gorczyca, T. W., Korista, K. T., et al. 2005a, A&A, 440 1203
Zatsarinny, O., Gorczyca, T. W., Korista, K. T., et al. 2005b, A&A, 438, 743
Zatsarinny, O., Gorczyca, T. W., Korista, K. T., Badnell, N. R., & Savin, D. W. 2003, A&A, 412, 587
Zatsarinny, O., Gorczyca, T. W., Korista, K. T., Badnell, N. R., & Savin, D. W. 2004a, A&A, 417, 1173
Zatsarinny, O., Gorczyca, T. W., Korista, K. T., Badnell, N. R., & Savin, D. W. 2004b, A&A, 426, 699